JOURNAL OF MATERIALS SCIENCE 24 (1989) 439–446

Debonding of photoresist caused by Case II diffusion

PETER J. MILLS*, EDWARD J. KRAMER
Department of Materials Science and Engineering and the Materials Science Center, Bard Hall, Cornell University, Ithaca, New York 14853, USA

A glassy polymeric photoresist bonded to a thin copper substrate was immersed in an organic penetrant environment. Debonding of the polymer layer from the substrate was observed by monitoring the deflection of the composite strip. The diffusion of the environment into the polymer layer was followed using Rutherford backscattering spectrometry. For all environments investigated the diffusion showed the characteristics of Case II diffusion, i.e. a uniformly swollen layer formed behind a sharp front and propagated into the polymer at a constant velocity. Even though the front velocity could be varied over three orders of magnitude by varying the environment or the temperature, debonding always occurred when the front had penetrated only about one-fifth of the total layer thickness. It is concluded that debonding is driven by release of the elastic strain energy stored in the composite strip rather than a specific attack of the interface by the environment. Additions of a smaller organic molecule to a predominately large organic molecule environment were found to produce a marked increase in the kinetics of debonding and a corresponding increase in the Case II front velocity. To discover the mechanism of this effect, experiments were carried out with mixtures of iodomethane and 1,1,1-trichloroethane (TCE). Rutherford backscattering spectra showed that the smaller iodomethane diffused ahead of the main Case II diffusion front of the TCE. It is proposed that the increase in Case II front velocity in the mixture results from the fact that the faster diffusing iodomethane preplasticizes the polymer ahead of the front.

1. Introduction

Debonding of a polymeric photoresist from the underlying material it is designed to protect as a result of exposure to organic environments is a topic of some technological interest. Such debonding of the resist upon exposure to the organic developer is catastrophic, but after it has served its purpose, the debonding of the resist in an organic "stripper" is desirable as a method of resist removal. In this paper we demonstrate that the debonding of a commercial dry film photoresist, Riston (trademark of E. I. du Pont de Nemours and Co.), in various organic environments is caused by the stresses developed ahead of a swollen layer that propagates into the polymer at a constant velocity. This non-Fickian mode of diffusion is known as Case II diffusion [1–13] and is characterized by an abrupt front ahead of which the concentration of the organic environment ("penetrant") decreases sharply. Behind the front the swollen polymer is rubbery and the concentration gradient of the penetrant is negligible. In our experiments we measure both the front velocity by Rutherford backscattering spectrometry (RBS) and the debonding time and show that under a wide variety of conditions debonding occurs when the front has propagated about one-fifth of the way through the polymer coating.

The principal penetrant investigated was 1,1,1-trichloroethane (TCE). However, when attempts were made to repeat the measurements with other batches of TCE, the specific values of the debonding times could vary by as much as a factor of three. These differences in debonding time were matched by corresponding differences in the Case II front velocity measured by RBS. Commercial TCE is frequently used as a degreasing agent for metals so additives are usually added to it to retard metal catalysed reactions. A possible explanation of the variation in debonding time therefore could be that the kinetics of Case II diffusion are very sensitive to the presence and concentration of these additives.

To show that this hypothesis is true we undertook further debonding measurements with solutions from a single batch of TCE where the additive concentration was reduced by aqueous extraction. Additives of smaller molecular size were found to increase the velocity of the Case II diffusion front by as much as an order of magnitude. Using RBS we were able to investigate the mechanism by which these additives alter the diffusion kinetics.

2. Experimental procedure

The Riston, which is a commercial dry film photoresist manufactured by DuPont, was obtained as 60 μm thick sheets and cross-linked by ultraviolet radiation. The

---

*Present address: Department of Materials Science and Engineering, University of Surrey, Guildford, Surrey, UK.

0022-2461/89 $03.00 + .12

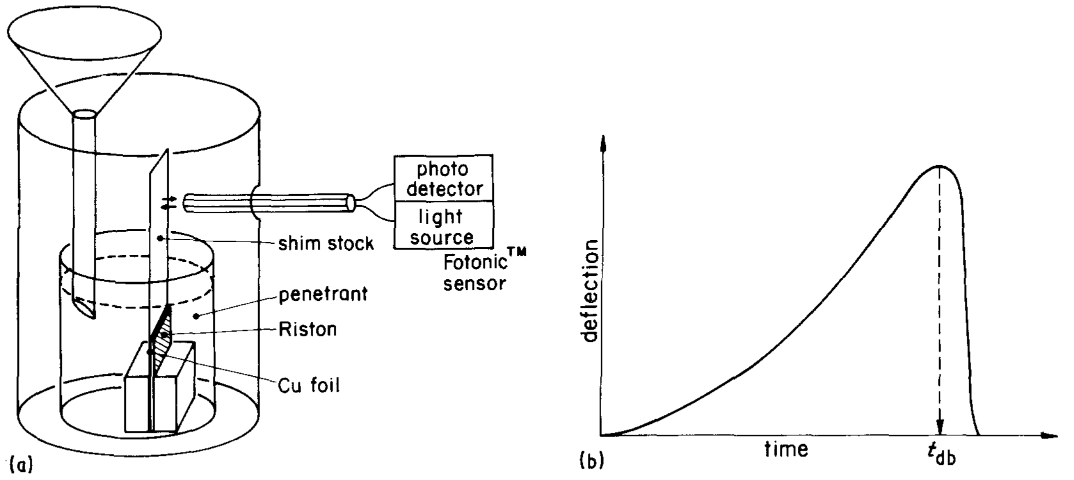

Figure 1 (a) Drawing of the apparatus for the debonding experiment. (b) Schematic drawing of a typical deflection–time curve showing debonding.

resist had a glass transition temperature, T_g, just below 60° C and a nominal composition as determined by RBS close to that of polymethylmethacrylate (PMMA). The resist was bonded to a thin copper foil. Samples of this bilayer film approximately 1 cm × 1 cm were clamped over the bottom 1/2 cm to a tall strip of thin metal shim stock (with the copper side facing the shim stock) and then placed in a beaker filled with sufficient penetrant that the polymer was completely immersed. The geometry is shown schematically in Fig. 1. As the polymer swells the bilayer film bent into a curve with the centre of curvature towards the side opposite the polymer surface causing the shim stock to deflect. The deflection of the shim stock was measured using a Fotonic (Mechanical Technology Inc, Latham, New York) sensor. The probe of this device consisted of two sets of optical fibres that were displaced with respect to one another. One set transmits light to the shim stock and the other collects the light reflected from it. If the end of the probe was initially held further from the reflecting surface than the spacing between the sending and receiving fibre bundles, a displacement of the reflecting surface (shim stock) away from the probe caused a decrease in received intensity. This intensity was measured by a photocell whose output provided a signal which was a measure of the deflection. The apparatus was enclosed in a sealed container which allowed the temperature to be controlled to $\pm 1°$ C.

The TCE was obtained from Fisher Scientific. The procedure used for extracting the small molecule additives involved shaking equivalent volumes of the TCE and distilled water for 2 min in a separation funnel. After the organic layer was separated it was dried with calcium sulphate which was then removed by filtration.

A detailed description of both the theory of RBS [14] and the experimental techniques developed for measuring concentration profiles of TCE and iodoalkanes in Riston may be found elsewhere [15]. Spectra consisting of the yield of backscattered He^{2+} ions versus their energy were obtained using an He^{2+} beam of incident energy 2.4 MeV directed at normal incidence to the sample surface. A simulated spectrum [16, 17] for the case where the front has advanced to a depth of 1 μm below the surface is shown in Fig. 2. The swollen layer has been assumed to contain a uniform concentration of the penetrant, in this case 0.1 weight fraction TCE and 0.01 weight fraction iodomethane, the latter to simulate the presence of a small molecule additive to TCE. The energies of the ions scattered from the surface carbon, oxygen, chlorine and iodine nuclei are indicated. Ions reaching the detector from each nucleus with lower than those energies were scattered from below the surface, with a larger energy loss corresponding to a greater depth. If present individually, chlorine and iodine can be probed to a depth of ~2 and ~4 μm, respectively, before the spectra from each of these nuclei begin to overlap with that from the oxygen from the surface of the polymer. But what makes the technique so ideal for this study is that the diffusion of an iodine-containing molecule can still be monitored independently in the presence of the chlorine-containing TCE to a depth of ~2 μm.

The Case II front depth after several exposure times was determined by matching the observed RBS spectrum with a simulated RBS spectrum like that in Fig. 2 from different thickness layers of swollen polymer; the front velocity was determined by fitting a straight line to the front depth against time data.

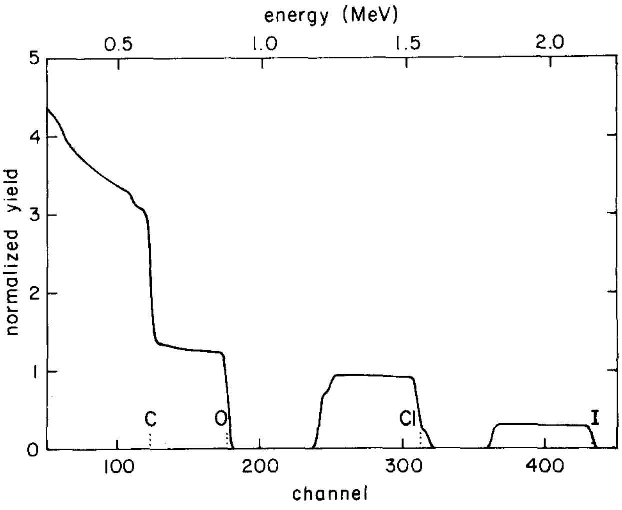

Figure 2 Simulated RBS spectrum from Riston after a uniformly swollen surface layer 1 μm thick containing 0.1 weight fraction TCE and 0.01 weight fraction iodomethane has formed by Case II diffusion.

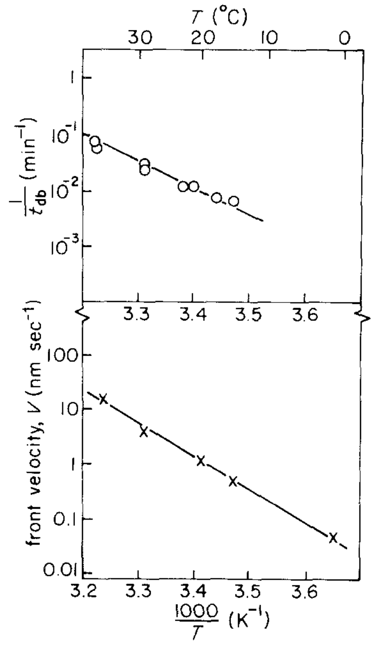

Figure 3 (a) Reciprocal of the debonding time in TCE as a function of reciprocal temperature. (b) Case II diffusion front velocity as measured by RBS as a function of reciprocal temperature.

3. Results

Fig. 1b shows schematically a deflection against time curve from the debonding experiment. As long as the swollen polymer layer remains in contact with its copper backing the bilayer sample continues to curl, leading to an increasing deflection as a function of time. When debonding begins, however, the deflection reaches a maximum and rapidly falls to zero as the elastically bent copper foil returns to its unstressed shape. A convenient measure of the debonding time is the time to the maximum deflection, t_{db}, as shown on Fig. 1b.

While one might imagine many possible causes of debonding, such as lateral attack of the polymer–copper interface, that do not depend on the Case II diffusion-controlled swelling of the polymer, these can be ruled out by showing that the inverse debonding time correlates very well with the velocity of the Case II diffusion front measured by RBS. Fig. 3a shows a plot of the logarithm of the inverse debonding time in TCE against $1/T$. It can be seen that the slope of this plot is almost the same as that of the plot of the logarithm of the Case II front velocity against $1/T$ shown in Fig. 3b. The activation enthalpy for debonding is close to, but slightly lower than, that for the front velocity.

If the hypothesis that Case II diffusion is responsible for the debonding is correct, the magnitude of the debonding time should be comparable to, but less than, the time, t_f, that the Case II front would require to propagate the entire 60 μm thickness of the film at the velocity determined by RBS. The solid triangles in Fig. 4 show the comparison of t_{db} with t_f over the range in temperature in Fig. 3; t_{db}/t_f is between 0.25 and 0.15. Debonding occurs when the TCE front has propagated approximately one-fifth of the total thickness of the polymer film. The relationship between Case II diffusion and debonding was observed for other organic swelling agents for the polymer. Fig. 4 also shows as crosses the t_{db} and t_f data for a homologous series of iodoalkanes, ranging from iodomethane (the smallest t_{db}) to iodohexane (the largest t_{db}). Again there is a direct correlation between the debonding time in the iodoalkane and the time that it would take the Case II diffusion front to traverse the polymer film.

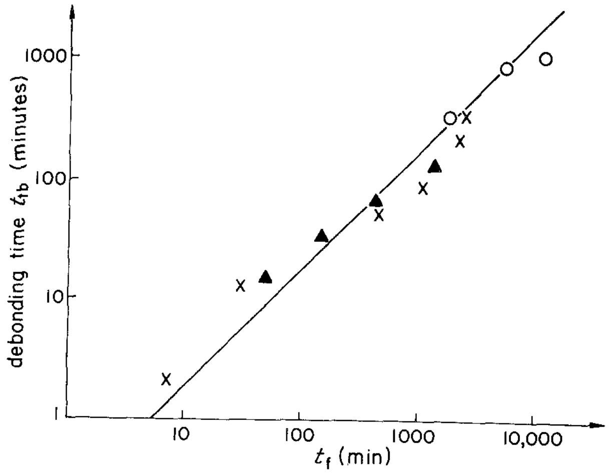

Figure 4 Debonding time plotted against t_f, the time it would take the Case II diffusion front to propagate entirely across the Riston film thickness. (▲) TCE at various temperatures, (○) TCEs from which the water soluble additives have been progressively extracted, (x) a homologous series of iodoalkanes ranging from iodomethane to iodohexane.

Table I shows the composition of the TCE used for these experiments as determined by gas chromatography. Note that besides the TCE there are small mole fractions of small molecule additives such as nitromethane, 1,2 dioxolane and methylethylketone. When these additives are progressively extracted with distilled water, the debonding time increases dramatically, as illustrated by the debonding times in Table II and the three open circles in Fig. 4, which correspond to the debonding in TCE after one, three and six water extractions. At first sight it would seem improbable that the increase in debonding time produced by extracting the small molecule additives could be due to a decrease in the velocity of the Case II diffusion front, especially given the small quantities of the additives involved. However, when the front velocity in the various water-extracted TCEs was measured, it was observed to decrease dramatically as more extractions were performed. In addition, the values of t_f and t_{db} for the water-extracted TCEs shown in Fig. 4 fall approximately on the same line established for the experiments using iodoalkanes and the TCE exposures at different temperatures.

If the hypothesis that the shorter debonding time of the polymer resist on exposure to the unextracted TCE is due to the presence of the small molecule

TABLE I Composition of TCE

Molecule	Mole fraction
1,1,1 trichloroethane	0.906
Nitromethane	0.023
1,3 dioxolane	0.021
Methylethyketone	0.014
Isobutanol	0.012
Toluene	0.012
1,2 epoxybutane	0.007
Ethylene dicholoride	0.002

TABLE II Debonding time of Riston in TCE after extraction

Penetrant	Debonding time (sec)
TCE as-received	240
TCE after 1 extraction	330
TCE after 3 extractions	887
TCE after 6 extractions	1067

additives, the debonding time should decrease further if small molecules are deliberately added to the unextracted TCE. Fig. 5 shows the results of just such an experiment in which various amounts of an additive, either methanol, iodomethane, iodoethane or 1-iodobutane were added. The debonding time decreases rapidly when small amounts of methanol are added, somewhat less rapidly when iodomethane is added, even less rapidly when iodoethane is added and only marginally when iodobutane is added. The effectiveness of an additive in decreasing the debonding time of the polymer film on exposure to TCE seems to correlate with the debonding time of the film in the pure additive which itself correlates well with molecular size. Fig. 6 shows a plot of the debonding time of the polymer film in various pure additives against their molecular volumes. Those additives which have a molecular volume much less than TCE, produce fast debonding of the polymer film and are particularly effective in decreasing the debonding time of the polymer as additives to the TCE. Because it is well known that the front velocity in Case II diffusion increases rapidly as the size of the penetrant decreases, and in particular for the homologous series of iodoalkanes in Riston [18], the fact that debonding time decreases with the size of the penetrant is expected. Those additives that are larger than TCE have Case II front velocities in the polymer that are lower than that of TCE, have longer debonding times and are relatively ineffective in decreasing the debonding time as additives.

Based on the results presented above it seems clear that the decrease in the debonding time of the polymer coating as small molecules are added to the TCE is due to an increase in the Case II diffusion front velocity. To understand the mechanism of that increase in front velocity, we used Rutherford backscattering spectrometry to follow both the TCE and the additive under circumstances where the Case II front velocity is much faster with the additive than without it. A solution of 0.19 mole fraction iodomethane in TCE is a useful example. The addition of the iodomethane decreases the debonding time (and increases the Case II front velocity) by about a factor of four as shown on Fig. 5. Figs 7a and b show the relevant portion of the RBS spectrum from the polymer film after exposure to the TCE–iodomethane solution for 30 and 60 sec, respectively. The energies 2.12 and 1.52 MeV) of He^{2+} ions scattered from iodine and chlorine nuclei at the surface are marked. The large increase in scattering just below 1.52 MeV is due to scattering from the chlorine nuclei behind the TCE Case II diffusion front. The decrease in scattering at energies less than 1.4 MeV after the 30 sec exposure and 1.2 MeV after the 60 sec exposure is due to the decrease in TCE (and chlorine nuclei) in the polymer glass just ahead of the front. The solid line is the simulated spectrum from a layer uniformly swollen with TCE, 325 nm thick after 30 sec and 850 nm thick after 60 sec.

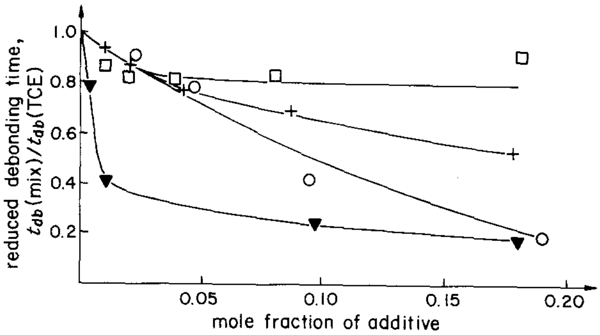

Figure 5 Reduced debonding time plotted against mole fraction of small molecule additive to TCE. Additives: methanol (▲), iodomethane (○), iodoethane (×), 1-iodobutane (□).

There is additional scattering in these spectra, at energies between 1.8 and 2.0 MeV for the sample exposed for 30 sec and between 1.6 and 1.8 for the sample exposed for 60 sec. This scattering is too high in energy to come from chlorine in the TCE or from carbon or oxygen in the polymer and can only come from iodine in the iodomethane. Note, however, that the main increase in this scattering does not occur just below the surface in the region that is highly swollen by TCE, but from a deeper layer that is just ahead of the main Case II front. This is a layer approximately 600 nm thick, starting 425 nm below the surface after 30 sec and 850 nm below the surface after 60 sec. The solid lines in Fig. 7 show the simulated spectra from layers swollen with iodomethane at these depths and thicknesses. The iodomethane concentration in the main layer swollen by the TCE (behind the main Case II front) is about three times lower than that in the 600 nm layer ahead of the front and the simulation includes the iodomethane in this region as well. It is worth noting that the concentration of iodomethane in the region ahead of the front is quite low, approximately 0.007 iodomethane molecules per PMMA mer compared with ~0.3 TCE molecules per PMMA mer behind the front. Nevertheless the TCE front velocity is increased substantially by the presence of this small amount of iodomethane ahead of the front as can be seen in Fig. 8 which shows the position of the TCE front after various times of exposure to TCE without and with the addition of iodomethane. Also shown is the position of the deepest penetration of the iodomethane. In all cases this position is about 600 nm ahead of the TCE front.

4. Discussion

4.1. Additive effects on Case II diffusion

In this section we discuss the mechanism by which small molecule additives affect the diffusion front velocity in the context of the model of Case II diffusion proposed by Thomas and Windle [13]. Case II diffusion is a mode of transport in which the swelling and diffusion are coupled to the chemically-driven mechanical deformation of the polymer glass. The deformation is dependent on the osmotic pressure which drives the swelling and on the deformation resistance

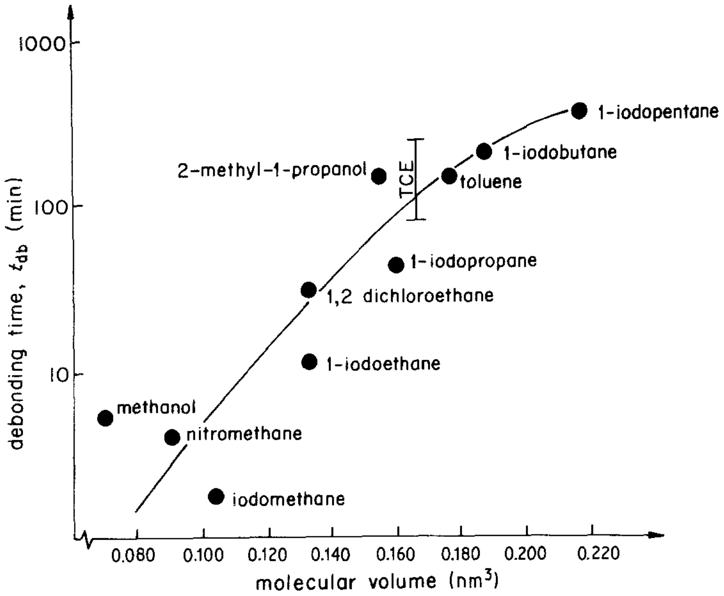

Figure 6 Debonding time as a function of molecular volume for various small organic molecules at 25° C.

(viscosity) of the polymer. Both the viscosity and diffusivity are extremely sensitive to the volume fraction ϕ, of the penetrant, with very large decreases in viscosity and large increases in diffusivity occurring in a narrow range of ϕ. These changes are probably due both to the plasticization caused by the sorption of the penetrant and to the swelling deformation itself, which "rejuvenates" (reverses the physical ageing of) the polymer glass. Both processes lead to a decrease in polymer segmental relaxation times from very large (glassy behaviour) to very short (rubbery behaviour). The strong dependence of viscosity and diffusivity on penetrant volume fraction produces the propagation of the sharp front that is characteristic of Case II diffusion.

A straightforward extension [15, 19, 20] of the Thomas and Windle model leads to a simple expression for the Case II front velocity, V

$$V = \left\{ D(\phi_m) \frac{a'(\phi_m)}{a(\phi_m)} \left[\frac{\partial \phi}{\partial t} \right]_{\phi_m} \right\}^{1/2} \qquad (1)$$

where $D(\phi_m)$ is the diffusivity of the penetrant in the glass, $a(\phi_m)$ and $a'(\phi_m)$ are the penetrant activity and its derivative with respect to ϕ, and $\partial\phi/\partial t$ is the swelling rate. All these quantities are to be evaluated at the maximum in osmotic pressure ahead of the front which occurs at the volume fraction of penetrant ϕ_m. To a good approximation, if ϕ_m is small (measurements in both the photoresist and polystyrene systems suggest that $\phi_m \approx 0.1$), $a(\phi_m)/a'(\phi_m) \approx 1/\phi_m$ so that Equation 1 can be rewritten as

$$V = \left\{ \frac{D(\phi_m)}{\phi_m} \left[\frac{\partial \phi}{\partial t} \right]_{\phi_m} \right\}^{1/2} \qquad (2)$$

Equation 2 has been shown to predict accurately the Case II front velocities of various iodoalkanes in polystyrene using values of D and $\partial\phi/\partial t$ determined from independent experiments [21].

One expects that both the diffusivity, D, and the swelling rate $\partial\phi/\partial t$ of the glass immediately ahead of

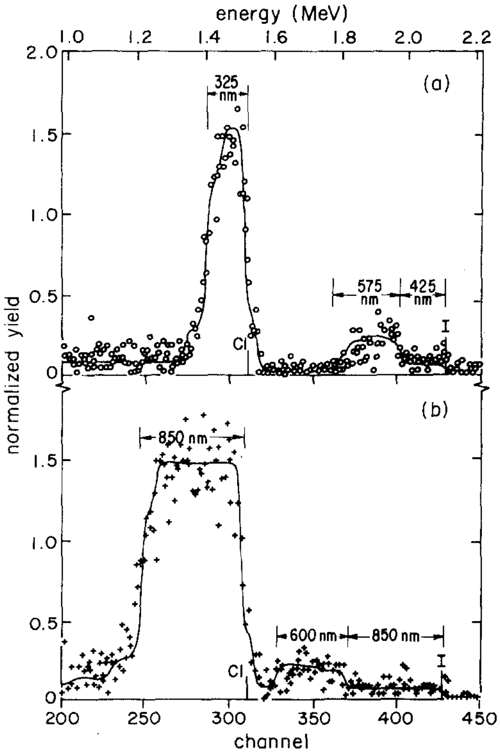

Figure 7 Rutherford backscattering spectra for Riston after exposure to TCE containing 0.19 mole fraction idomethane additive. (a) Exposure time 30 sec. (b) Exposure time 60 sec.

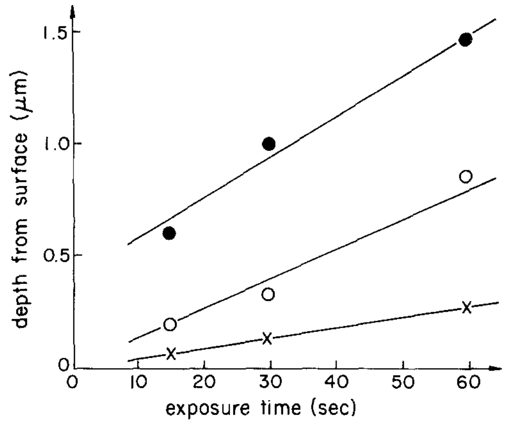

Figure 8 Depth of the TCE Case II diffusion front from the surface of TCE without iodomethane additive (x), and with 0.19 mole fraction iodomethane additive (O). (●) Depth of the iodomethane diffusion below the surface for the TCE with 0.19 mole fraction additive.

the front should depend on the glass transition temperature of the polymer there. In particular, a decrease in T_g of the polymer should produce a rapid increase in the swelling rate. In the model of Thomas and Windle the plasticization effect of the penetrant is taken into account explicitly by assuming that the swelling is linear viscous with a viscosity, η, which varies as

$$\eta = \eta_0 \exp(-m\phi) \tag{3}$$

where m is a constant which depends on the plasticizing efficiency of the penetrant [13]. The swelling rate in the Thomas and Windle model thus becomes

$$\frac{\partial\phi}{\partial t} = \frac{P}{\eta_0} \exp(m\phi) \tag{4}$$

where P is the osmotic pressure ($P \approx \ln(\phi_e/\phi)$ where the subscript e represents the value of ϕ that would be in local equilibrium).

In our experiments there are at least two molecules diffusing which are capable of causing plasticization: the penetrant TCE and the small molecule additive(s). The swelling rate in this instance should be

$$\frac{\partial\phi}{\partial t} = \frac{P}{\eta_0} \exp(m\phi) \exp\left(\sum_i m_i\phi_i\right) \tag{5}$$

where the subscript i denotes each additive species. Thus if the small molecule additives can diffuse ahead of the front they can be expected to strongly increase the swelling rate there. Similar effects of the small molecule additives on D of the penetrant also can be expected; moreover, the increases in the swelling rate will decrease ϕ_m, the volume fraction of TCE at the maximum in the osmotic pressure.

Thus each of the factors that determine the Case II front velocity in Equation 2 is affected by the small molecule additives in such a way as to increase V. The apparent mechanism of these additives is to "preplasticize" the polymer ahead of the front. The strong effect of additive size (Fig. 6) is probably due both to the fact that only smaller molecules whose Case II diffusion is faster than that of TCE can outrun the TCE front and preplasticize the glass ahead of it and to the fact that the smaller molecules are more efficient plasticizers than the larger ones.

The higher concentration of the iodoalkanes ahead of the TCE front is another interesting feature of these results. This enhanced concentration could reflect an increase in the equilibrium solubility of the small iodoalkanes ahead of the front due to the triaxial tension that exists there. On the other hand, it could be simply due to a decrease in the solubility of the iodoalkanes behind the front in the region of high TCE concentration. The latter hypothesis seems the most likely but at the moment there is no way to test which of these hypotheses is correct.

4.2. Debonding and Case II diffusion

The results presented above clearly show that the debonding of the polymer film from the copper substrate is controlled by the propagation of the Case II diffusion front. Alternative explanations such as direct attack of the interfacial bond between the polymer film and the copper can be ruled out by the excellent correlation observed between t_{db} and t_f for a wide variety of conditions and penetrants. Nevertheless, we observe that debonding occurs not when the Case II front has traversed nearly the entire thickness of the film but only approximately one-fifth of it. We believe that this observation provides an important clue that the debonding is driven by the release in elastic energy stored in the swollen layer behind the front.

The elastic energy G released per unit area when a crack propagates in the interface between the Riston and the copper depends approximately quadratically on both the depth x_f of the swollen layer and the volume swelling strain ε_s in the material behind the front, i.e.

$$G = A\,\varepsilon_s^2 x_f^2 \tag{6}$$

where A is a parameter which depends on the elastic moduli of the Riston both ahead of and behind the front as well as elastic modulus and thickness of the copper film. The derivation of Equation 6 and the details of A are given in the Appendix. Debonding is predicted to occur when G exceeds the critical strain energy release rate (fracture toughness G_{Ic}) of the interface [22, 23], i.e. when

$$x_f \geqslant (G_{Ic}/A\,\varepsilon_s^2)^{1/2} \tag{7}$$

The estimate of $A = 1.2 \times 10^{10}\,\mathrm{J\,m^{-4}}$ at debonding given in the Appendix leads to a reasonable value of $0.071\,\mathrm{J\,m^{-2}}$ for G_{Ic} in TCE using the experimentally determined values of $x_f \cong 12\,\mu\mathrm{m}$ and $\varepsilon_s \cong 0.2$. Equation 7 also predicts that the x_f at debonding will be approximately constant if G_{Ic}, A and ε_s are approximately constant, a prediction that is in good agreement with the observation that the photoresist film debonds when the Case II front has reached approximately the same depth below the surface. As can be inferred from Fig. 4, x_f is not completely independent of temperature showing a modest decrease at higher temperatures. Indeed a temperature dependence is expected, because G_{Ic}, A and ε_s should show some changes with temperature. The swelling strain, ε_s, might also be expected to be different for different solvents and G_{Ic} should vary from solvent to solvent as a consequence of the different interfacial energies between different solvents and the debonded surfaces. However, in this case, RBS measurements of the ε_s indicate that the variation in ε_s is small and Fig. 4 demonstrates that x_f is approximately constant here as well. The large variation in debonding time from one iodoalkane to another is therefore due entirely to the large variation in the Case II front velocity with molecular size.

5. Conclusions

1. Debonding of the polymer layer in organic environments is caused by the elastic energy stored in the film due to a swollen outer layer which forms by a Case II diffusion mechanism.

2. The kinetics of debonding are thus determined largely by the velocity of the Case II diffusion front. Factors which increase the front velocity, such as

small molecule additives, also decrease the debonding time by the appropriate factor.

3. Small molecule additives can markedly increase the velocity of the Case II diffusion front, apparently by "preplasticizing" the glass ahead of the front.

Acknowledgements

The primary support of this research by IBM is gratefully acknowledged. We also acknowledge the use of the facilities of the Cornell Materials Science Center which is funded by the National Science Foundation, Division of Materials Research, Materials Research Laboratories Program. We appreciate the enthusiastic guidance of Professor J. W. Mayer on all aspects of RBS and the able experimental assistance of John Fitch. We also thank Phil Isaacs for performing the gas chromotography on the TCE.

Appendix

We outline here the calculation of the strain energy release rate, G, for a partially swollen polymer film from an elastic substrate with a Young's modulus, E_s. The swollen film of total thickness, L, consists of an outer rubbery layer of Young's modulus, E, and thickness, x_f, and an inner glassy layer of Young's modulus, E_g, and thickness $L - x_f$. The magnitude of the moduli of the various layers are such that $E_s \gg E_g \gg E$. Consider a crack which is just beginning to propagate along the interface parallel to the length of a strip of width b of the film and substrate. The swelling of the outer layer causes the uncracked strip to bend and an elastic energy, W_0, per unit length to be stored. After the crack has propagated along the interface the strip, which loses its stiff substrate, bends to a higher curvature but retains some stored elastic energy, W_f, per unit length. Because the strain energy release rate $G = (W_0 - W_f)/b$, the problem can be reduced to computing W_0 and W_f. The first step is to compute the biaxial stress, σ_s, in the rubbery layer due to the swelling in the absence of any bending of the beam. This stress is $\sigma_s = -E\varepsilon_s/3(1 - \nu)$ where ν is Poisson's ratio of the rubber. As $\nu \cong 0.5$, $\sigma_s = -2E\varepsilon_s/3$. This stress gives rise to a moment, M, given by

$$M = -\sigma_s K \qquad \text{(A1)}$$

where $K = 0.5\,bx_f(x_1 + x_2)$ and where x_1 and x_2 are the distances from the neutral axis of the beam to the outer and inner surfaces of the swollen layer, respectively. The moment, M, causes the beam to bend and a normal strain, $\varepsilon(x)$, to arise parallel to the length of the beam given by

$$\varepsilon(x) = Mx/(EI) \qquad \text{(A2)}$$

where x is the distance from the neutral axis and I is the effective moment of inertia of the beam. To compensate for the different moduli of the different layers of the beam this effective moment of inertia is to be computed for a beam whose width varies as its modulus, i.e. $b(x) = bE(x)/E$. The normal stress in the unswollen regions of the beam is thus

$$\sigma(x) = ME(x)x/(EI) \qquad \text{(A3a)}$$

and in the swollen region

$$\sigma(x) = ME(x)x/(EI) + \sigma_s \qquad \text{(A3b)}$$

In principle one must correct the moment for the relaxation of the swelling stress due to the bending of the beam so that

$$M = -K\sigma_s\{1 + [\mathrm{K}(x_1 + x_2)/2I]\} \qquad \text{(A4)}$$

but for the case of interest to the paper, i.e. $E_s \gg E_g \gg E$, this correction is small and can safely be ignored. Another simplification which arises due to the large differences in moduli is that the neutral axis lies to a very good approximation on the neutral axis of the highest modulus layer alone, i.e. at the mid-thickness of the substrate for the film plus substrate and at the mid-thickness of the polymer glass layer for the debonded film.

The energy stored per unit length, W, is given by,

$$W = b \int \mathrm{d}x \int_0^{\sigma(x)} \mathrm{d}\sigma\, \varepsilon(x), \qquad \text{(A5)}$$

which can be written as

$$W = bx_f E\, \varepsilon_s^2/[9(1 - \nu)] - (1 - \nu)M^2/(2EI) \qquad \text{(A6)}$$

While the first term in Equation A6 does not change as a result of the debonding, the second term is changed both by a decrease in M and a large decrease in I and thus the strain energy release rate is given by

$$G = (W_0 - W_f)/b$$
$$= -[Ebx_f^2\varepsilon_s^2/18(1\text{-}\nu)]\, \Delta[(x_1 + x_2)^2/4I] \qquad \text{(A7)}$$

or

$$G = Ax_f^2\varepsilon_s^2 \qquad \text{(A8)}$$

where

$$A = -[Eb/18(1\text{-}\nu)]\, \Delta[(x_1 + x_2)^2/4I],$$

and where $\Delta(\ )$ represents the change in the quantities inside the brackets as a result of debonding. For the estimate of A in the text, L and x_f were taken as 60 and 12 μm, respectively, the thickness of the copper substrate as 18 μm, and thus $x_1 = 69\,\mu$m and $x_2 = 57\,\mu$m before debonding and 36 and 24 μm after debonding. The Young's moduli of the various layers were taken as $E_s = 124\,000$ MPa, $E_g = 124$ MPa and $E = 12.4$ MPa, which leads to values of I before and after debonding for a 1 m wide strip of 54.8×10^{-13} m^4 and 0.93×10^{-13} m^4, respectively.

References

1. T. ALFREY, *Chem. Eng. News* **43** (1965) 64.
2. A. C. NEWNS, *Trans. Faraday Soc.* **52** (1956) 1533.
3. G. S. PARK, in "Diffusion in Polymers", edited by J. Crank and G. S. Park (Academic, London, 1968) p. 141.
4. H. B. HOPFENBERG, R. H. HOLLEY and V. STANNETT, *Polym. Engng Sci.* **9** (1969) 242.
5. R. H. HOLLEY, H. B. HOPFENBERG and V. STANNETT, *ibid.* **10** (1970) 376.
6. B. R. BAIRD, H. B. HOPFENBERG and V. STANNETT, *ibid.* **11** (1971) 274.
7. C. H. M. JACQUES, H. B. HOPFENBERG and V. STANNETT, *ibid.* **13** (1973) 81.
8. G. SARTI, *Polymer* **20** (1979) 827.
9. N. L. THOMAS and A. H. WINDLE, *Polymer* **18** (1977) 1195.
10. *Idem, J. Membrane Sci.* **3** (1978) 337.

11. *Idem, Polymer* **21** (1980) 619.
12. *Idem, ibid.* **22** (1981) 627.
13. *Idem, ibid.* **23** (1982) 529.
14. W. K. CHU, J. W. MAYER and M. A. NICOLET, "Backscattering Spectrometry" (Academic, New York, 1978) Ch. 1.
15. P. J. MILLS, C. J. PALMSTRØM and E. J. KRAMER, *J. Mater. Sci.* **21** (1986) 1479.
16. L. R. DOOLITTLE, *Nuclear Instrum. Meth.* **B9** (1985) 344.
17. *Idem, ibid.* **B15** (1986) 227.
18. P. J. MILLS and E. J. KRAMER, *J. Mater. Sci.* **21** (1986) 4151.
19. C.-Y. HUI, K. C. WU, R. C. LASKY and E. J. KRAMER, *J. Appl. Phys.* **61** (1987) 5137.
20. *Idem,* MSC Report no. 5851, *ASME Trans,* in press.
21. R. C. LASKY, PhD thesis, Cornell University (1986) p. 119.
22. K. KENDALL, "Electronic Packaging Materials Science", Materials Research Society Symposium Proceedings, Vol. 40, edited by E. A. Giess, K.-N. Tu, D. R. Uhlmann (Materials Research Society, Pittsburgh, Pennsylvania, 1985) p. 167.
23. *Idem, J. Phys. D Appl. Phys.* **6** (1973) 1782.

Received 11 January
and accepted 9 May 1988